The Effect of Nitrate Availability on Oxygen Isotope Fractionation During Cyanobacterial Photosynthesis

Lingkun Guo

Senior Honors Thesis

Advised by Dr. Laurence Yeung

Department of Earth, Environmental and Planetary Sciences

Rice University

2023

Abstract

Marine primary productivity supports food webs and ecosystem health, driving large-scale animal distribution patterns in the ocean. Primary productivity is also a fundamental process in the biological pump, which sequesters inorganic carbon from the atmosphere through photosynthesis and transports it to the ocean interior where it can be stored for millennial or greater timescales. Presently, different methods for quantifying productivity disagree with each other, presenting a major research challenge. To understand how climate change may impact the biosphere, it is necessary to continuously improve methods for quantifying primary productivity. The isotopic composition of dissolved oxygen in the ocean can be used as a constraint on oxygen production and therefore, be used to quantify marine primary productivity through the carbon-oxygen stoichiometry of photosynthesis. To distinguish newly produced O_2 from O_2 already present in the atmosphere, the $^{18}O/^{16}O$ and $^{17}O/^{16}O$ ratios of dissolved oxygen can be used. This approach is termed the "triple-oxygen isotope (TOI) method" and it relies on laboratory studies of the behavoir of oxygen isotope ratios during photosynthesis to constrain field measurements. Despite the potential of the TOI method, major knowledge gaps remain. For example, nutrient availability affects the photosynthesis activity of microorganisms and is heterogeneous across global oceans. Therefore, understanding how oxygen isotope fractionation may vary under nutrient stress is crucial for correctly interpreting field measurements. To address this knowledge gap, this study examines the effect of nitrate availability on the isotopic composition of cyanobacterial photosynthetic oxygen. Freshwater cyanobacteria *Synechocystis* PCC 6803 are inoculated in media with different nitrate concentrations. The cyanobacterial photosynthetic oxygen is collected and its TOI composition is analyzed. Additionally, this study generates new data on the clumped isotope composition of photosynthetic oxygen, which is a parameter describing the degree of randomness in the distribution of rare oxygen isotopes (^{17}O and ^{18}O) in O_2 molecules. Results suggest that there is larger oxygen isotope fractionation when cyanobacteria experience more nitrate limitation, and that the TOI and clumped isotope composition of photosynthetic oxygen can be utilized together to constrain gross oxygen production and provide information on the mechanism of cyanobacterial photosynthesis.

Contents

1 Background and Motivation **2**

1.1 Methods of Primary Productivity Quantification 2

1.2 Triple Oxygen Isotope Method 3

1.3 Clumped Isotope Composition 5

1.4 Nitrogen Usage by Cyanobacteria 6

1.5 Light-Dependent Oxygen Consuming Reactions 7

1.6 Motivation 7

2 Methods and Materials **8**

2.1 Cyanobacteria Incubation 8

2.2 Experiment Set-Up 8

2.3 Photosynthesis Experiment Process 10

2.4 Sample Analysis 10

3 Results **11**

3.1 TOI Composition of Cyanobacterial Photosynthetic Oxygen 11

3.2 Effect of Nitrate Availability on Fractionation Factors 12

3.3 Clumped Isotope Composition of Cyanobacterial Photosynthetic Oxygen 13

4 Discussion **14**

4.1 Nitrate Availability and Light Level Both Affect Intracellular Redox Conditions 14

4.2 Impact of Nitrate Availability on Estimates of Oxygen Production 16

4.3 Clumped Isotope Composition of Photosynthetic Oxygen 18

4.4 Analogy to Real-World Environmental Conditions 18

5 Conclusion **20**

6 Acknowledgements **21**

References **22**

Background and Motivation

Marine primary productivity supports food webs and ecosystem health, driving large-scale animal distribution patterns in the ocean (Hunt and McKinnell, 2006). It is also a fundamental process in the biological pump, which sequesters inorganic carbon from the atmosphere through photosynthesis and transports it to the ocean interior where it can be stored for millennial or greater timescales. The biological pump is crucial for regulating the carbon cycle and climate, and its efficiency has been predicted to weaken due to global warming (Sigman and Boyle, 2000; Yamamoto et al., 2018). Biogeochemical models that simulate the rate and dynamics of the biological pump, marine food webs, and other important processes in the biosphere all rely on accurate quantification of primary productivity (Nowicki et al., 2022). Therefore, it is necessary to continue to develop and improve methods for quantifying primary productivity, especially for the purpose of understanding how future climate change may impact the biosphere.

1.1 Methods of Primary Productivity Quantification

Primary productivity can be described by the chemical reaction in which inorganic carbon is reduced and converted into organic carbon while water is oxidized and transformed into oxygen.

$$CO_2 + H_2O \xrightarrow{h\upsilon} O_2 + CH_2O \tag{1}$$

Various tools exist to quantify primary productivity, including bottle incubation experiments, satellite remote sensing, and models based on isotopic mass balance (Luz and Barkan, 2000). Each of these methods measures a different component of the primary productivity equation.

The bottle incubation method using radioactive carbon labelling was first proposed by Nielsen (1952) who added ^{14}C-labeled sodium bicarbonate to seawater samples and measured the abundance of ^{14}C in organic matter after incubation. The advantages of this method include its high sensitivity and the relative ease to generate a large amount of data (Marra, 2009). However, there are also concerns raised about the bottle incubation method. This method may be subject to bias due to the "bottle effect" in which isolating samples in bottles may alter the trophic compartments and interactions of marine phytoplankton. The bottle effect may introduce disagreements on primary productivity measurements from the smaller microbiological scale to the larger biogeochemical scale (Elena García-Martín et al., 2011). It is also ambiguous whether this method measures gross

primary production, net primary production, or something in between (Marra, 2009). Alternatively, the bottle incubation method using ^{18}O-labeled H_2O in addition to ^{14}C incubation could improve the estimates of primary productivity (Bender et al., 1999). However, the ^{18}O method is still subject to the uncertainties introduced by the bottle effect (Quay et al., 2010).

Satellite remote sensing may also be utilized to quantify primary productivity by the measurement of ocean color (Lee et al., 2015). This method measures the CH_2O component in the primary productivity equation in which higher productivity results in a larger quantity of chlorophyll being present in the ocean, which can be detected by remote sensing. Chlorophyll measurements are then inputted into productivity methods to compute time- and depth-integrated primary production (Behrenfeld and Falkowski, 1997). The method has the unique benefit of providing greater spatial and temporal coverage than *in situ* measurements and allowing for observations in locations that are difficult for *in situ* sampling, such as the Arctic Ocean (Hill et al., 2013). Uncertainties of the remote sensing method come from inconsistencies among ocean-color models that utilize satellite measurements to predict global primary productivity, especially under conditions of high nutrient, low chlorophyll, and extreme temperatures (Carr et al., 2006).

1.2 Triple Oxygen Isotope Method

Triple-oxygen isotope (TOI) analysis of O_2 can be used as a constraint on oxygen production and therefore, be used to quantify primary productivity (Luz and Barkan, 2005; Juranek and Quay, 2013). The TOI method relies on the observation that biological processes including photosynthesis and respiration produce $\delta^{17}O$ and $\delta^{18}O$ values that plot along a line with a mass-dependent slope (Luz and Barkan, 2000). Meanwhile, stratospheric photochemical reactions result in mass-independent isotope fractionation. The effects of stratospheric reactions, respiration, and evapotranspiration cause atmospheric O_2 to have an anomaly in ^{17}O relative to water in the ocean (Luz et al., 1999; Young et al., 2014). This anomaly is described by the TOI parameter $\Delta'^{17}O$, which is the measure of the departure in a substance's isotopic composition from the expected composition that is predicted by a mass-dependent relationship (Ash et al., 2020).

$$\Delta'^{17}O = \ln(\delta^{17}O + 1) \quad \ln(\delta^{18}O + 1) \times \lambda \tag{2}$$

In the equation above, λ is the reference slope that denotes the empirically determined mass-dependent relationship between $\delta^{17}O$ and $\delta^{18}O$ values due to respiration and air-sea gas exchange. Typically, the value $\lambda_{respiration} = 0.518$ is used in calculations of marine oxygen production (Luz and Barkan, 2009; Juranek and Quay, 2013). However, the empirical value of $\lambda_{respiration} = 0.522$ has also been proposed (Ash et al., 2020). Figure 1 is a graphical representation of the TOI method. The $\delta^{17}O$ and $\delta^{18}O$ composition of dissolved O_2 is plotted on the dashed line representing the mixture between atmospheric and photosynthetic O_2. Respiration affects the composition of dissolved O_2 by causing it to move along the line with a slope that equals to $\lambda_{respiration}$.

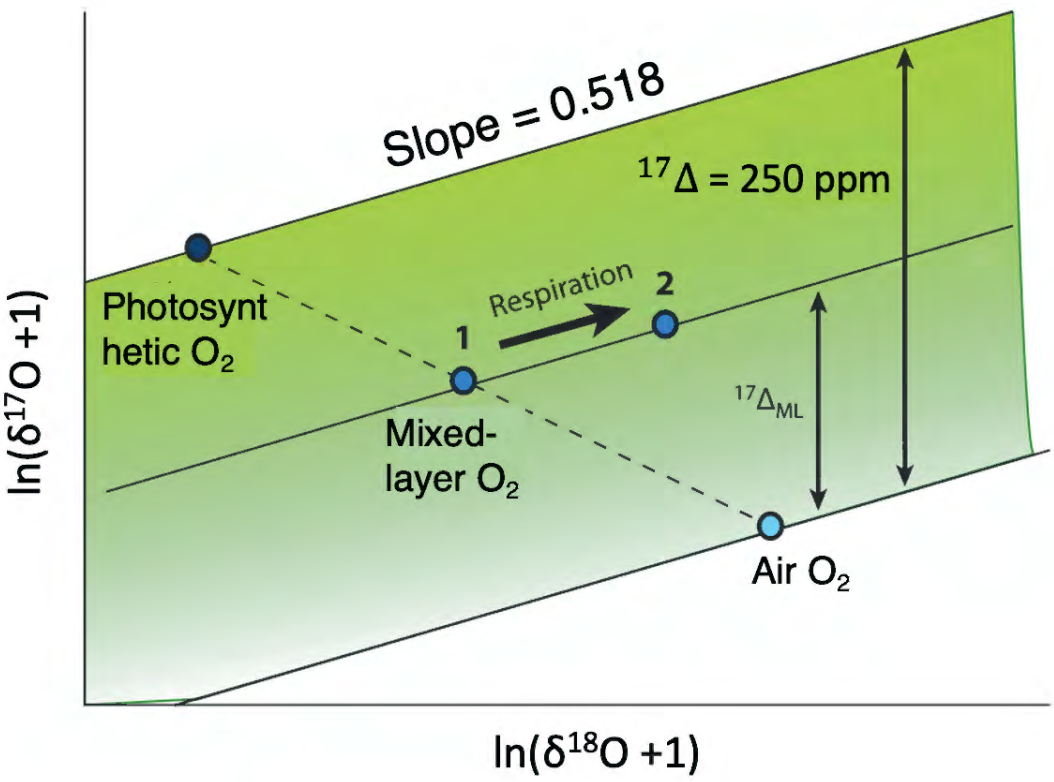

Figure 1. Schematic (after Juranek and Quay (2013)) depicting the principles of the TOI method. The horizontal and vertical axis are the amount of fractionation of ^{18}O and ^{17}O relative to the source water, respectively. The reference slope λ is assumed to have a value of 0.518.

At steady-state, a triple-oxygen isotope mass balance can be constructed for dissolved O_2 in the ocean's mixed layer, which allows for gross oxygen production (GOP) to be calculated using the following equation from Prokopenko et al. (2011). The TOI method has the benefit of being incubation-independent, which means that the amount of GOP derived from this equation reflects the productivity of plankton communities under natural conditions, integrated over the residence

time of dissolved O_2 in the mixed layer (Juranek and Quay, 2013).

$$\frac{G}{kO_{eq}} = \frac{\frac{^{17}R_{dis}\ \ ^{17}R_{eq}}{^{17}R_{eq}} \quad \lambda \frac{^{18}R_{dis}\ \ ^{18}R_{eq}}{^{18}R_{eq}}}{\frac{^{17}R_p\ \ ^{17}R_{dis}}{^{17}R_{dis}} \quad \lambda \frac{^{18}R_p\ \ ^{18}R_{dis}}{^{18}R_{dis}}} \tag{3}$$

1.3 Clumped Isotope Composition

Clumped isotope composition of O_2 is described by the parameters Δ_{35} and Δ_{36}; these parameters quantify the extent to which ^{17}O and ^{18}O are randomly distributed among all isotopologues of O_2. Δ_{35} and Δ_{36} values are defined by the amount of $^{17}O^{18}O$ and $^{18}O^{18}O$ in the sample, measured against the stochastic distribution of these two multiply-substituted isotopologues in which there are more than one rare isotope in the molecule. If Δ_{35} and Δ_{36} have values of zero, this indicates that the distribution of ^{17}O and ^{18}O in the sample is random. Positive or negative values of Δ_{35} and Δ_{36} indicate enrichment or depletion of the multiply-substituted isotopologues (Eiler, 2007).

The clumped isotope composition of photosynthetic O_2 has not been previously measured directly, but its value has been computed from theory (Yeung et al., 2015; Yeung, 2016). The Δ_{35} and Δ_{36} parameters of photosynthetic O_2 represent the relationship between two different and independent isotope fractionation factors corresponding to the two water-splitting reactions that occur in the oxygen-evolving complex in Photosystem II. The Δ_{36} parameter expressed specifically for photosynthesis is derived by Yeung et al. (2015):

$$\Delta_{36,p} = \frac{\alpha_A \alpha_B}{\frac{1}{4}(\alpha_A + \alpha_B)^2} \quad 1 \tag{4}$$

α_A and α_B are the isotope fractionation factors associated with the two water-binding sites in the Oxygen Evolving Complex of Photosystem II. The fractionation factors are independent from each other. Based on the equation above, if the difference between α_A and α_B is small, then the value of Δ_{36} will approach zero; if the difference is large, then the value of Δ_{36} will be a negative number. Therefore, the expected clumped isotope composition of photosynthetic O_2 is equal to or less than zero (Yeung, 2016).

Because clumped isotope compositions are concerned with the ordering of heavy isotopes and not the bulk isotopic composition in a sample, this parameter has the benefit of being independent of the bulk isotopic composition of the substrate, such as the water in which photosynthetic organisms

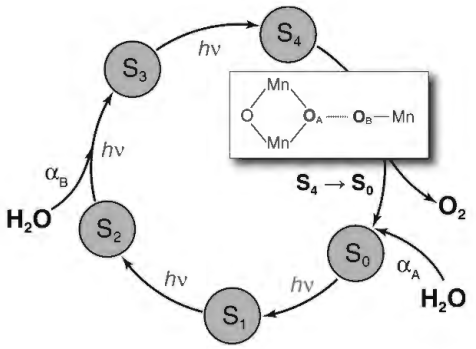

Figure 2. Schematic of the Oxygen Evolving Complex of Photosystem II. Figure from Yeung et al. (2015).

are growing (Eiler, 2007). This unique benefit potentially allows the clumped isotope composition of O_2 to act as an independent tracer of photosynthesis and supplement the triple oxygen isotope method to quantify marine primary productivity. Atmospheric O_2 have Δ_{35} and Δ_{36} values of 1‰ and 2‰ (Yeung et al., 2014). Similar to the TOI signature, the contrast between the clumped O_2 signature of photosynthetic and atmospheric O_2 can be utilized to constrain gross primary productivity.

1.4 Nitrogen Usage by Cyanobacteria

Nitrogen is an important nutrient for cyanobacteria growth and its concentration can vary locally and seasonally (Andersen et al., 2020; Hutchins and Fu, 2017). Inorganic nitrogen, including nitrite, nitrate, and ammonium, has been shown to limit bacterial growth during the boreal spring in the Atlantic Ocean, whereas co-limitation by organic carbon and inorganic nitrogen is observed during boreal autumn (Hale et al., 2017). Nitrogen is also the limiting nutrient for phytoplankton growth in the oligotrophic waters of the tropical western North Pacific (Li et al., 2015). The marine cyanobacteria species *Prochlorococcus* experiences nitrogen stress in the Indian Ocean and co-stress from nitrogen and phosphorus limitation in the tropical and South Atlantic (Ustick et al., 2021). In freshwater systems, phosphorus is the primary limiting nutrient, while nitrogen provides secondary limitation during late summer and fall (Moon and Carrick, 2007).

Cyanobacteria possess genes coding for nitrate assimilation, which allows intracellular nitrate to be reduced to nitrite and ammonium by nitrate reductase. Nitrate assimilation is a crucial process in non-N_2-fixing cyanobacteria. After nitrate reduction, the intracellular ammonium is incorporated into the carbon skeletons of organic nitrogen compounds (Flores and Herrero, 2005). The nitrate reduction process in cyanobacteria is also closely related to photosynthesis in which water photolysis

can generate the energy necessary to reduce nitrate to nitrite then ammonium (Flores et al., 2005; Inabe et al., 2021).

Ammonium is preferred over nitrate during inorganic nitrogen assimilation by cyanobacteria. The freshwater cyanobacteria species *Synechocystis* sp. strain PCC 6803 is shown to grow at a higher rate and attain higher cellular biomass when supplied with 5 mM of NH_4Cl rather than 5 mM of $NaNO_3$. This is because nitrate assimilation requires the rate-limiting process of nitrate reduction, while ammonium assimilation does not require additional energy for reduction (Flores and Herrero, 2005). Ammonium is much less abundant than nitrate in the ocean; therefore, most phytoplankton possess nitrate reductase, which allows the organism to utilize nitrate as a nitrogen source (Capone et al., 2008).

1.5 Light-Dependent Oxygen Consuming Reactions

Previous studies on oxygen isotope fractionation during photosynthesis show that the water-splitting reaction occurring in Photosystem II does not fractionate oxygen isotopes; the enrichment in heavy oxygen isotopes observed during photosynthesis occurs due to light-dependent oxygen consuming reactions, such as the Mehler-like reaction in cyanobacteria (Eisenstadt et al., 2010; Helman et al., 2005; Barkan and Luz, 2011). The Mehler-like reaction is a photoprotective mechanism that reduces O_2 and H^+ to H_2O. The flavodiiron proteins Flv1 and Flv3 direct electron flow from NADPH to O_2. (Allahverdiyeva et al., 2015; Lea-Smith et al., 2016). The Flv1 and Flv3 proteins are crucial to *Synechocystis* survival under fluctuating light conditions, which are common in aquatic environments (Allahverdiyeva et al., 2013).

It has been shown that nutrient limitation in *Chlamydomonas reinhardtii* may activate photoprotective responses that alleviates excitation pressure from Photosystem II (Saroussi et al., 2017). Since the Mehler-like reaction in cyanobacteria is a form of photoprotective response, it is likely to also be affected by nutrient limitation. We expect that an increase in the occurrence of Mehler-like reactions would result in larger observed oxygen isotope fractionation. We hypothesize that photosynthetic O_2 has a triple-oxygen isotopic composition different from that of the growth media and that environmental stress has an impact on this isotopic composition.

1.6 Motivation

Biogeochemical models use experimental data on oxygen isotope fractionation by various processes and isotopic mass balance to quantify oxygen productivity. A strong understanding on

the fractionation caused by different endmembers of biogeochemical processes is necessary to correctly constrain the models. However, previous studies on the triple oxygen isotopic signature of photosynthetic O_2 did not account for the potential effect of environmental stress (e.g., low nutrient availability) on oxygen isotope fractionation. Measurements of $\delta^{17}O$ and $\delta^{18}O$ values were all produced from bacteria cultures grown with excess nutrients (Helman et al., 2005; Eisenstadt et al., 2010). It is important to understand how nutrient concentration may affect the isotopic composition of photosynthetic oxygen because this information will elucidate the effect of photosynthesis on the isotopic composition of dissolved oxygen in natural waters. If environmental stress does affect the extent of oxygen isotope fractionation by photosynthesis, then this effect must be accounted for by biogeochemical models in order to yield accurate estimates of primary productivity.

This study investigates the impact of nitrate availability on oxygen isotope fractionation during cyanobacterial photosynthesis. The result of this study are new measurements of the $\delta^{17}O$, $\delta^{18}O$, $^{17}\Delta$, and Δ_{36} values of photosynthetic O_2. The first three parameters serve as a re-evaluation of the triple-oxygen isotope fractionation by photosynthesis and elucidate the effect of nutrient stress on oxygen isotope fractionation. Additionally, this project yields new data on the clumped-isotope composition of photosynthetic O_2, which are used to evaluate whether the Δ_{36} parameter can serve as an independent tracer for quantifying primary productivity.

Methods and Materials

2.1 Cyanobacteria Incubation

Cells of the freshwater cyanobacteria *Synechocystis* sp. strain PCC 6803 (hereafter *Synechocystis*) were grown in the freshwater BG-11(-N) medium at pH 7.5 supplemented with varying concentrations of $NaNO_3$ (Stanier et al., 1971). These cultures were grown at 33°C under a light intensity of 100 μmol photons m^{-2} s^{-1} with a 12/12 hr light/dark period. They were incubated in a Benchmark Incu-shaker at 180 revolutions/minute.

2.2 Experiment Set-Up

When the cyanobacteria cultures had reached an absorbance of 0.1-0.2 as measured on the Thermo Scientific Aquamate 8100 UV-Visible Spectrophotometer at 730 nm, the cultures were transported to the turbo-pumped vacuum line for photosynthesis experiment. The experimental setup consisted of a vacuum line with four parts:

1. The reaction vessel containing the culture was kept at temperatures between 23-25°C . During collection, O_2 was continuously removed from the reaction vessel by bubbling of He at a flow rate of 500 mL min ^{1}.

2. Two cold traps were kept at temperatures of -7 - -5 °C and -30- -20°C . He carrier gas passed through the cold traps to remove water vapor from the system. Two additional cold traps were kept at -196°C , with the purpose of removing CO_2 from the system.

3. The collection U-trap was a stainless steel tube filled with silica gel and kept at -196°C which allowed O_2 to adsorb onto the silica gel while letting the He gas flow through the U-trap.

4. The sample finger contained silica gel and was kept at -196°C which was used for the final collection of O_2. It was then sealed with an O-ring and transferred to the gas chromatography line for analysis.

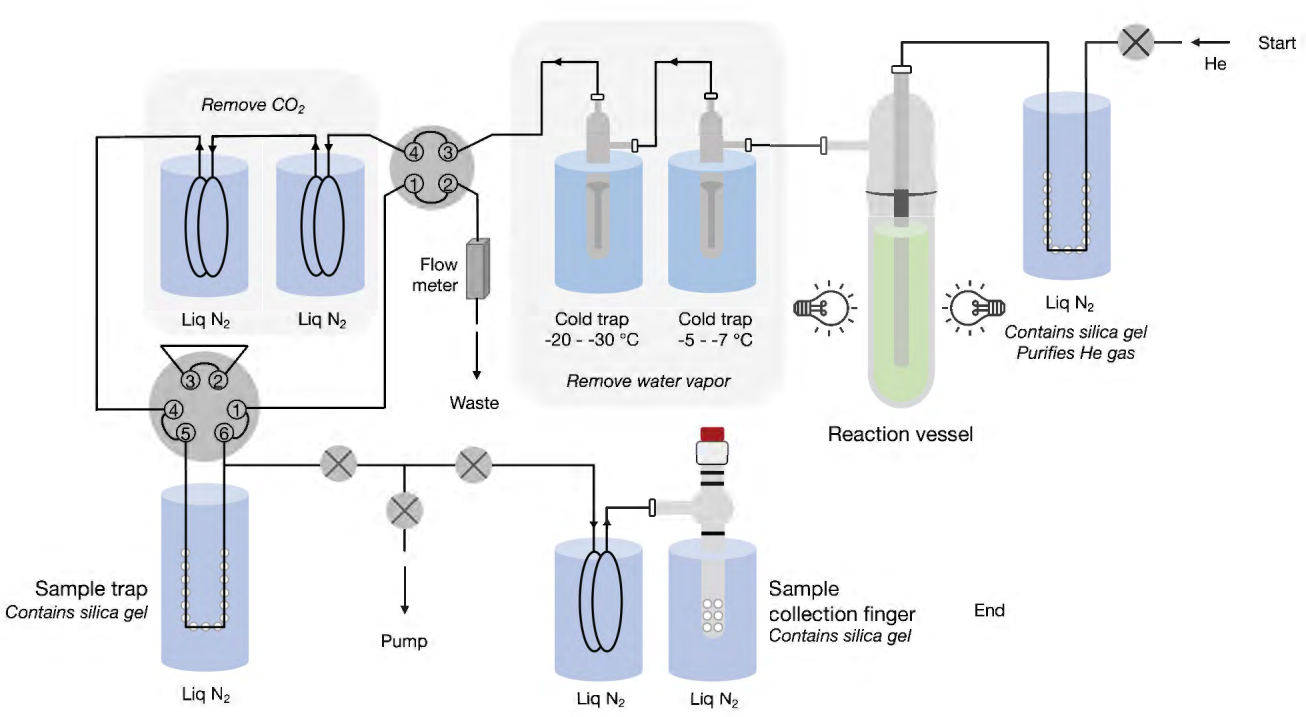

Figure 3. Schematic of photosynthesis experiment set-up.

2.3 Photosynthesis Experiment Process

At the beginning of each experiment, the culture was bubbled with He at 500 mL min^{-1} for 40 min to remove dissolved gases in the culture and air in the head space of the reaction vessel. During He-bubbling, the six-way valve was closed such that gases did not pass through the collection U-trap. Instead, the carrier He gas and gases being removed directly went to waste.

After 40 min of He-bubbling, the photosynthetic O_2 collection process began, which lasted for 2 hours. During this time, the lights on both sides of the reaction vessel supplied a constant light intensity. He flow was maintained at 500 mL min^{-1}. The six-way valve was opened to allow He gas and photosynthetic O_2 to flow through the collection U-trap that was kept at -196°C with liquid N_2. At this temperature, O_2 adsorbed onto the surface of silica gel and was kept in-place in the collection U-trap while He continued to flow through the system and go to waste.

At the end of photosynthetic O_2 collection, the six-way valve was closed to isolate the collection U-trap from the rest of the high-vacuum line. The valves between the collection U-trap and the turbo pump were opened slowly to pump out remaining He in the U-trap. Subsequently, the valve before the pump was closed, and the valves between the collection U-trap and the sample finger were opened. The collection U-trap was heated to 90°C while the sample finger was kept at -196°C . This temperature gradient allowed the photosynthetic O_2 sample to be transferred from the silica gel in the U-trap to the silica gel in the sample finger. The sample transfer process lasted for 45 min.

During the experiment, other oxygen-fractionating processes are highly restricted by the experimental conditions. Newly produced O_2 is immediately removed by He gas, which limits respiration and photorespiration from occurring. The lights used in experiments emit at wavelengths in the range of 420-780 nm, which does not include UV light. This minimizes the possibility of photo-oxidation of dissolved organic carbon (Sutherland et al., 2022). Oxygen isotope fractionation due to respiration, photorespiration, and photo-oxidation should be minimized during experiments. Therefore, the observed isotope fractionation in this study should only result from the Mehler-like reaction.

2.4 Sample Analysis

The O_2 collected in the sample finger was purified through gas chromatography, which allowed for the removal of Ar, N_2, and other trace gases from the sample. After purification, the sample was expanded into the sample bellows of the mass spectrometer. The sample was analyzed by a

high-resolution Nu Instruments *Perspective IS* isotope ratio mass spectrometer to determine δ^{33}, δ^{34}, and δ^{36} of the sample relative to the working gas (Ash et al., 2020; Yeung et al., 2018). For the first set of experiments (conducted at a light intensity of 1000 μmol photons m ^{2} s ^{1}), both the sample and the reference gas were measured at 40 nA in 6 blocks, each block consisting of 20 cycles of alternating measurements of the sample and reference gas. For the second set of experiments (conducted at a light intensity of 1300 μmol photons m ^{2} s ^{1}), the sample and the reference gas were measured at 8 nA, 20 nA, or 40 nA, depending on the amount of photosynthetic oxygen in the sample. Both the sample and the reference gas were measured for 6 blocks.

The δ^{18}O of the source water was measured using a Picarro L2130-i Cavity Ring-Down Spectrometer (CRDS) at Rice University. All runs were performed using a 3-point calibration using in-house materials (bottled water or lab tap) which were calibrated to Vienna Standard Mean Ocean Water (VSMOW, δ^{18}O = 0‰) and Standard Light Antarctic Precipitation (SLAP, δ^{18}O = -55.5‰). In-house calibration standards included Kona Deep (δ^{18}O = -0.3‰), Lab Tap 4 (δ^{18}O = -4.65‰) and Iceland Glacial (δ^{18}O = -8.09‰). One check standard was analyzed as an unknown for each run: USGS standard RSIL-67400 (δ^{18}O = -1.97‰) was always accurate to within $\pm$ 0.11‰. An in-house standard (Lab Tap 4) was used also as drift and memory effect corrections following the methods of (van Geldern and Barth, 2012). All data are normalized to Vienna Standard Mean Ocean Water (VSMOW).

Some nitrate was consumed during cyanobacteria inoculation. Therefore, the cultures were sampled after experiment and the final nitrate concentration was determined using the standard addition method. Nitrate concentration was measured on the ThermoFisher Scientific Dionex Integrion HPIC system using the Dionex IonPac AS25 column, which is a hydroxide selective anion exchange column.

Results

3.1 TOI Composition of Cyanobacterial Photosynthetic Oxygen

The fractionation factor of ^{17}O is plotted against that of ^{18}O in Figure 4, and the slope obtained from the data is $\lambda = 0.512 \pm 0.017$. Table 1 is a compilation of $\lambda_{Photosynthesis}$ values observed in previous studies on various phytoplankton species. The $\lambda_{Photosynthesis}$ value from this study is within the range of plausible values from previous studies. A paired t-test shows no statistically significant

difference between the $\lambda_{Photosynthesis}$ value reported in this study and the value of the TOI slope of the Mehler-like reaction performed by *Synechocystis* from Helman et al. (2005).

Previous Study	Organism	$\lambda_{Photosynthesis}$
Helman et al. (2005)	*Synechocystis* (Mehler-like Reaction)	0.497 ± 0.004
Eisenstadt et al. (2010)	*Chlamydomonas reinhardtii*	0.5198 ± 0.0001
	Nanochloropsis sp.	0.5253 ± 0.0004
	Phaeodactylum tricornutum	0.5234 ± 0.0004
	Emiliania huxleyi	0.5253 ± 0.0004

Table 1. Values of TOI slope generated by previous studies.

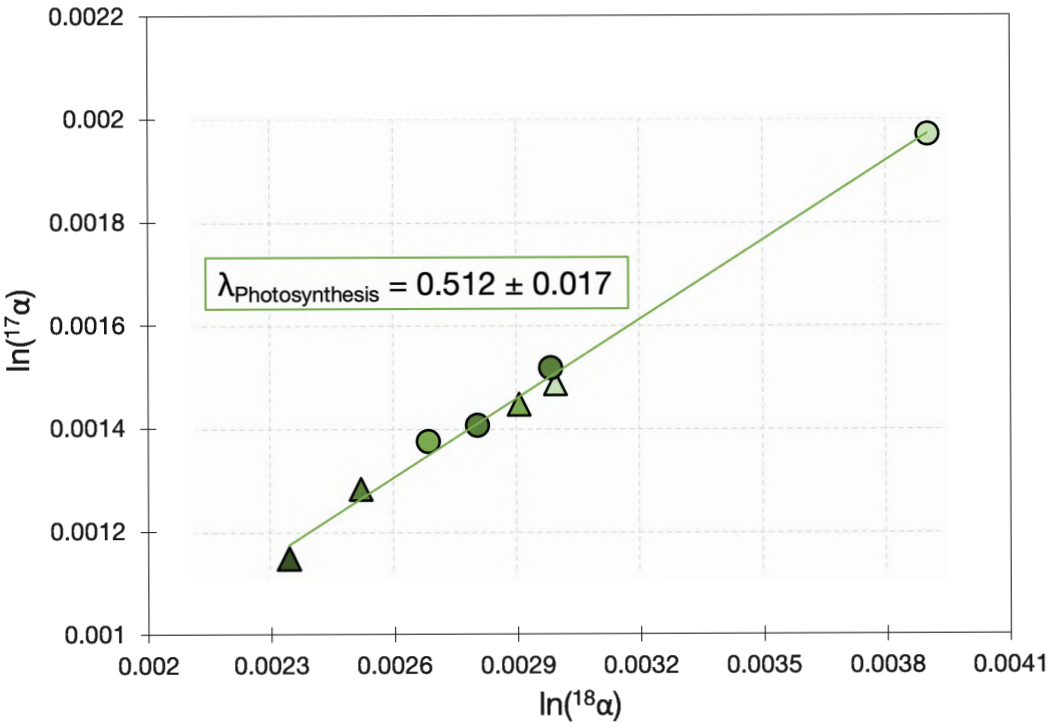

Figure 4. $ln(^{18}\alpha)$ and $ln(^{17}\alpha)$ values of cyanobacterial photosynthetic oxygen are plotted on the x and y axis, respectively. The slope of the regression line is denoted by the parameter $\lambda_{Photosynthesis}$. Data points in triangle markers represent experiments conducted at a light intensity of 1000 μmol photons m ^{2} s ^{1}. Data points in circle markers were generated at 1300 μmol photons m ^{2} s ^{1}. Darker colors of the marker represent higher concentrations of nitrate in the *Synechocystis* culture.

3.2 Effect of Nitrate Availability on Fractionation Factors

Figure 5 shows the effect of nitrate availability on the fractionation factors of ^{18}O. Oxygen isotope fractionation factors are generally higher for the samples collected at lower nitrate concentrations. This general trend is observed at two high light intensities. Two sets of experiments were conducted,

each under a different light intensity. At a light intensity of 1000 μmol photons m ^{2} s ^{1}, experiments were conducted at nitrate concentrations of 12.518 mM, 3.765 mM, 0.376 mM, and 0.003 mM. The maximum value of fractionation factor observed at this light level was $^{18}\alpha = 1.002912$, corresponding to the lowest nitrate concentration. There is no statistically significant difference between the fractionation factors at the two highest or the two lowest nitrate concentrations. At a higher light intensity of 1300 μmol photons m ^{2} s ^{1}, the maximum value of fractionation factor observed was $^{18}\alpha = 1.003909$. Experiments were conducted at nitrate concentrations of 3.741 mM, 2.753 mM, 0.067 mM, and 0.003 mM.

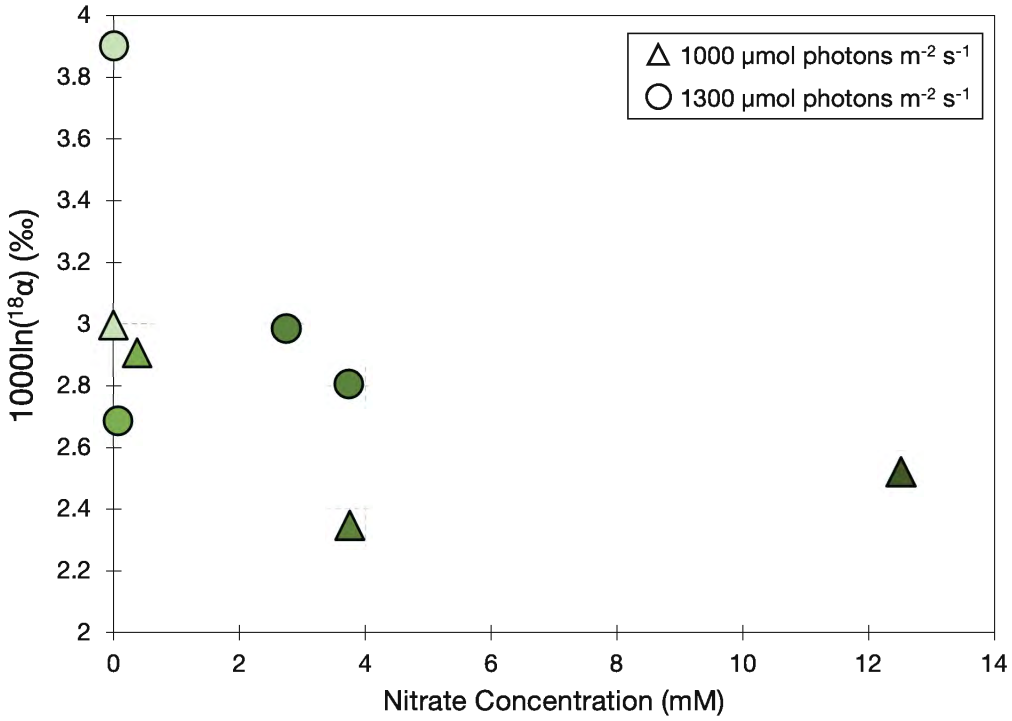

Figure 5. $^{18}\alpha$ values of *Synechocystis* photosynthesis are plotted against the nitrate concentration of the cultures. The triangle data points denote experiments conducted at a light intensity of 1000 μmol photons m ^{2} s ^{1}. The circle data points denote experiments conducted at a light intensity of 1300 μmol photons m ^{2} s ^{1}. Error bars of the data points are plotted but the magnitude of the error is smaller than the data point themselves.

3.3 Clumped Isotope Composition of Cyanobacterial Photosynthetic Oxygen

Figure 6 shows the Δ_{36} values of photosynthetic O_2 and their relationship with nitrate availability. There is no statistically significant difference between the Δ_{36} values at different nitrate concentrations. All Δ_{36} values fall between 0.10 0.01‰, and there is no significant difference between the highest value and $\Delta_{36} = 0$‰. The Δ_{36} was not measured for experiments conducted at a light

intensity of 1300 μmol photons m ^{2} s ^{1} because these experiments did not generate enough photosynthetic oxygen for clumped isotope analysis.

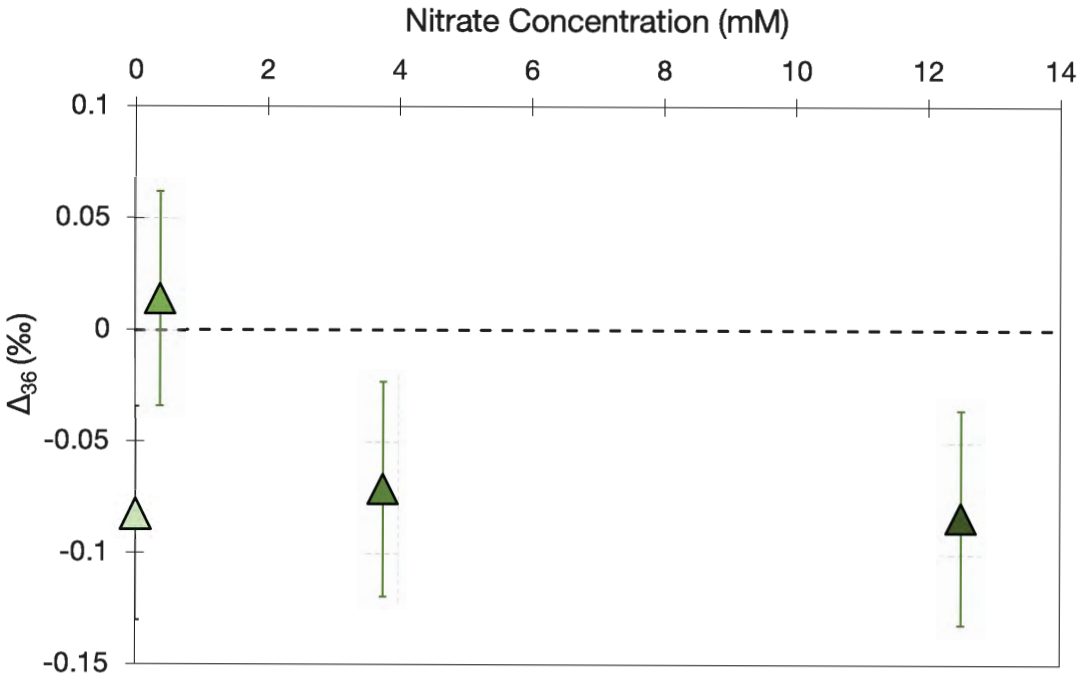

Figure 6. Δ_{36} values of photosynthetic O_2 generated by *Synechocystis*. The horizontal axis shows the concentration of nitrate (mM). All *Synechocystis* experiments plotted here were performed under a light intensity of 1000 μmol photons m ^{2} s ^{1}.

Discussion

4.1 Nitrate Availability and Light Level Both Affect Intracellular Redox Conditions

When cyanobacteria experience nitrogen limitation, there are changes in their intracellular redox state that result in reduced photosynthetic activity. For the non-diazotrophic cyanobacteria *Synechococcus elongatus*, nitrogen starvation generates metabolic signals as well as a redox signal. Nitrate and nitrite reductases act as electron sinks to avoid over-reduction of the cells (Klotz et al., 2015). Nitrogen limitation in *Synechocystis* is shown to induce over-reduction of the photosynthetic apparatus even under low light intensities due to a low availability of terminal electron acceptors. The observed responses in the cell include down-regulation of photosynthetic electron transport and degradation of the phycobilisome protein. The latter allows nitrogen to be reallocated to critical pathways in the cell (Salomon et al., 2013; Krasikov et al., 2012). These studies all show that nitrogen limitation affects cyanobacteria metabolism and photosynthetic activity by influencing the

intracellular redox state.

In addition to nutrient limitation, high light levels also result in intracellular oxidative stress. Cyanobacteria experience oxidative stress when reactive oxygen species (ROS), such as singlet oxygen, hydroxyl radical, superoxide anion, and hydrogen peroxide, are created at a rate faster than the rate at which they are broken down by the cell. ROS are produced when the amount of light energy received by photosystems exceeds the amount of energy consumed by cellular processes (Imlay, 2003; Muramatsu and Hihara, 2012; Rachedi et al., 2020). The response of cyanobacteria to high light level stress includes degradation of the light-harvesting phycobilisome protein, decrease in the amount of photosynthetic pigments, accumulation of light stress proteins, and O_2 reduction to H_2O by the Mehler-like reaction (Muramatsu and Hihara, 2012). Some of these response mechanisms overlap with those observed under nitrogen limitation. The similarity in response makes sense because high light levels and nitrogen limitation both exert stress on cyanobacteria by altering the intracellular redox state.

The changes in cyanobacteria electron transport chain under high light levels and nitrogen limitation stress are closely related to each other. While studies on the Mehler-like reaction primarily focus on how it responds to high light levels, it is likely that the reduction of excess O_2 to H_2O is a more general protective mechanism when cyanobacteria cells are under oxidative stress. It is reasonable to say that since nitrogen limitation makes cyanobacteria more vulnerable to over-reduction and photo-damage, there should be a higher dependence on the Mehler-like reaction as a photo-protective mechanism under nitrogen-limitation. More photosynthetic O_2 is reduced to H_2O during this up-regulation of the Mehler-like reaction. As a result, there is more observed enrichment in ^{17}O and ^{18}O in the residual O_2.

The relationship between different cellular responses to high light levels and nitrogen limitation stress is apparent when considering the paths of electron transfer during photosynthesis. As shown in Figure 7, photosynthetic electron transport in cyanobacteria takes place at the thylakoid membrane where the chlorophyll *a* pigment is energized by light at a wavelength of 680 nm and is subsequently oxidized by pheophytin. Electron is then transferred to plastoquinone, the cytrochrome bf complex, plastocyanin, and chlorophyll *a* in Photosystem (PS) I, in this order. After reaching PS I, the electron has several potential paths to follow. In the first potential path, the electron is transferred to phylloquinone, the Fe-S protein, then ferridoxin, which eventually directs the electron to the NADP reductase to produce NADPH. Alternatively, ferridoxin can direct the electron to plastoquinone,

which generates ATP (Chan, 2003). In the last potential path, the electron may be directed by PS I to reduce O_2 to H_2O as a part of the Mehler-like reaction (Allahverdiyeva et al., 2013). The ratio of electrons that is directed to each of the three paths depends on intracellular redox conditions and the level of oxidative stress experienced by the cell.

During the experiments performed in this study, cells of *Synechocystis* were subjected to stress due to both high light level and nitrogen limitation simultaneously. Distinguishing the response of cyanobacteria to each individual source of stress (i.e. light level, nitrogen limitation) is difficult without utilizing genetic tools such as suppressing the function of specific proteins. In one experiment, we attempted to only impose nitrogen limitation stress on the cells by performing the experiment at a light level of 60 μmol photons m^{-2} s^{-1}. However, the cells were not able to produce enough O_2 for analysis on the mass spectrometer. Nevertheless, the result of this study shows that under the same intensity of light level, the addition of nitrogen limitation stress causes *Synechocystis* to be more reliant on the Mehler-like reaction as a protective mechanism against oxidative stress.

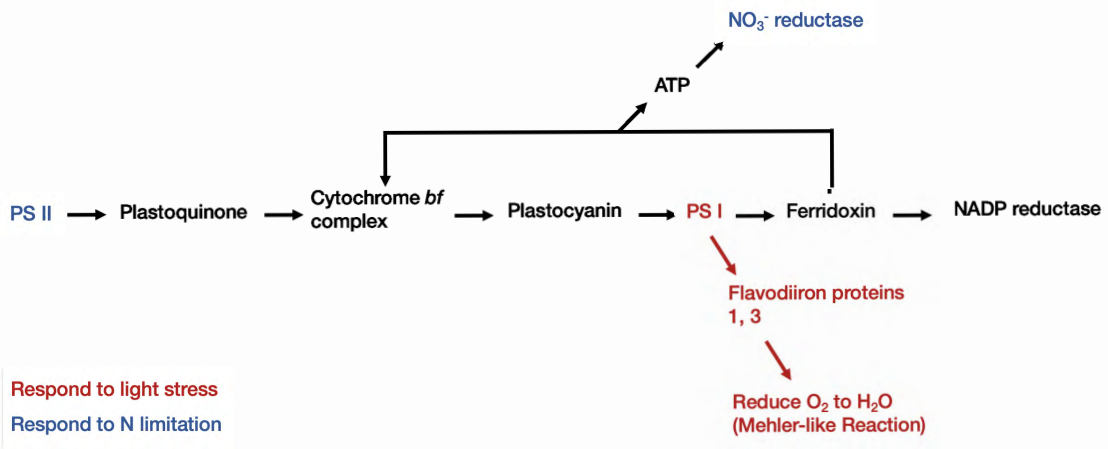

Figure 7. Schematic of electron transport during photosynthesis (after Chan (2003). Components in red text have been shown to respond to light level stress. Components in blue text have been shown to respond to nitrogen limitation stress.

4.2 Impact of Nitrate Availability on Estimates of Oxygen Production

Given the effect of nitrate availability on oxygen isotope fractionation factors at low nitrate concentrations, it is necessary to quantify the potential effect on the estimates of oxygen production. Figure 8 shows the range of gross oxygen production computed using Equation 3. The range of $^{18}\alpha$

used in this calculation comes from experiments with *Synechocystis*. The corresponding $^{17}\alpha$ values are computed using the slope of the regression line ($\theta_{17/18} = 0.536$) that is fitted to the data from *Synechocystis* experiments. Using the minimum and maximum values of $^{18}\alpha$ and $^{17}\alpha$ measured by this study, the resulting parameter representing the amount of gross oxygen production shows a 30.25% increase. This suggests that previous estimates of marine gross oxygen production using the TOI method were likely over-estimations under nitrate limitation.

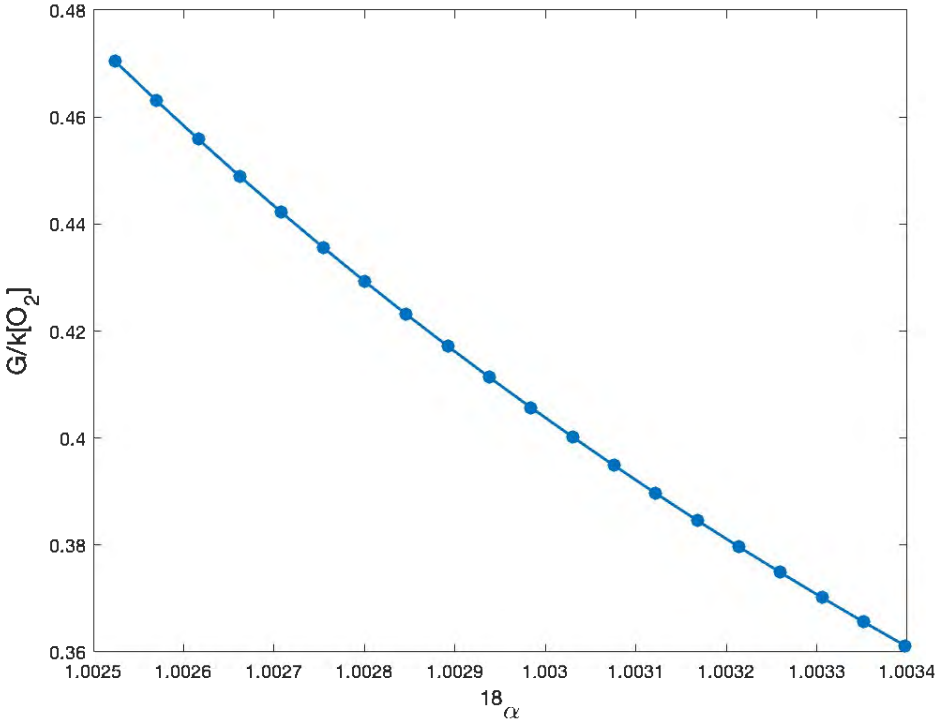

Figure 8. Calculations of gross oxygen production using Equation 3 (Prokopenko et al., 2011). The range of $^{18}\alpha$ observed in this study is used. The maximum and minimum values of $G/k[O_{eq}]$ are 0.4705 and 0.3612.

The expressed fractionation factor of oxygen isotopes during cyanobacterial photosynthesis depends on the condition of the cells, i.e. the level of intracellular stress they are experiencing due to nitrate limitation. Although the level of nutrient limitation stress increases with decreasing nitrate concentration in the medium, cells of cyanobacteria may exhibit similar behavior in a certain range of nitrate concentration. For example, the expressed fractionation factors were not significantly different between the two highest or two lowest nitrate concentrations in the experiments carried out at a light intensity of 1000 μmol photons m ^{2} s ^{1}. While the difference between the two highest nitrate concentrations is large (> 8 mM), the cells were not experiencing drastically different levels

of nutrient limitation stress. The small variations in cellular responses in this range are unlikely to be expressed as significant changes in oxygen isotope fractionation factors during photosynthesis.

4.3 Clumped Isotope Composition of Photosynthetic Oxygen

This study generates new data on the clumped isotope composition of cyanobacterial photosynthetic O_2, denoted by Δ_{36}. The Δ_{36} values observed in this study are consistent with that estimated by Yeung et al. (2015), which states that photosynthetic O_2 should have $\Delta_{36} \leq 0$. Since Δ_{36} remains constant under changing nitrate concentrations, the clumped isotope composition of dissolved O_2 can potentially serve as an independent constraint on oxygen production, which supplements the TOI method. The Δ_{36} parameter also has the unique benefit of being independent from the oxygen isotopic composition of the source water.

Figure 9 conceptually demonstrates how the Δ_{36} parameter can be used to constrain oxygen production. This approach is similar to that of the TOI method in which the Δ_{36} values of photosynthetic O_2 and air O_2 are empirically determined. Δ_{36} of photosynthetic O_2 is plotted at the origin because the results of this study show that it has a value close to 0‰. The value of the reference slope denoting the mass-dependent fractionation effect of respiration is empirically determined as $\lambda_{respiration} = 2.048$ by Ash et al. (2020). The value of the reference slope is computed based on the definition of the stochastic distribution of ^{18}O in O_2, and it has a value of $\lambda_{stochastic} = 2$. Photosynthetic O_2 is plotted at the origin because the result of this study shows that $\Delta_{36,photosynthesis} = 0$. The Δ_{36} value of dissolved O_2 in the ocean is a mixture between the two endmembers, photosynthetic O_2 and air O_2. Graphically, $\Delta_{36,ML}$ is the vertical distance between the point representing mixed layer O_2 and the stochastic distribution of ^{18}O in O_2 molecules. The fraction of contribution from each of the two endmembers can be determined using their respective Δ_{36} signature.

4.4 Analogy to Real-World Environmental Conditions

By subjecting cells of *Synechocystis* to nitrate limitation stress and high light levels, this study aims to replicate the environmental conditions that cyanobacteria experience in nature. In the low latitudes, light intensity at the surface ocean could be as high as 1700 μmol photons m^{-2} s^{-1} (Boswell et al., 2020). The realistic light levels are much higher than the experimental conditions of previous studies, which included light levels in the range of 40-250 μmol photons m^{-2} s^{-1} (Guy et al., 1993; Helman et al., 2005; Eisenstadt et al., 2010). Other experimental conditions also seek to achieve the purpose of reproducing realistic environmental conditions. Unlike previous studies such

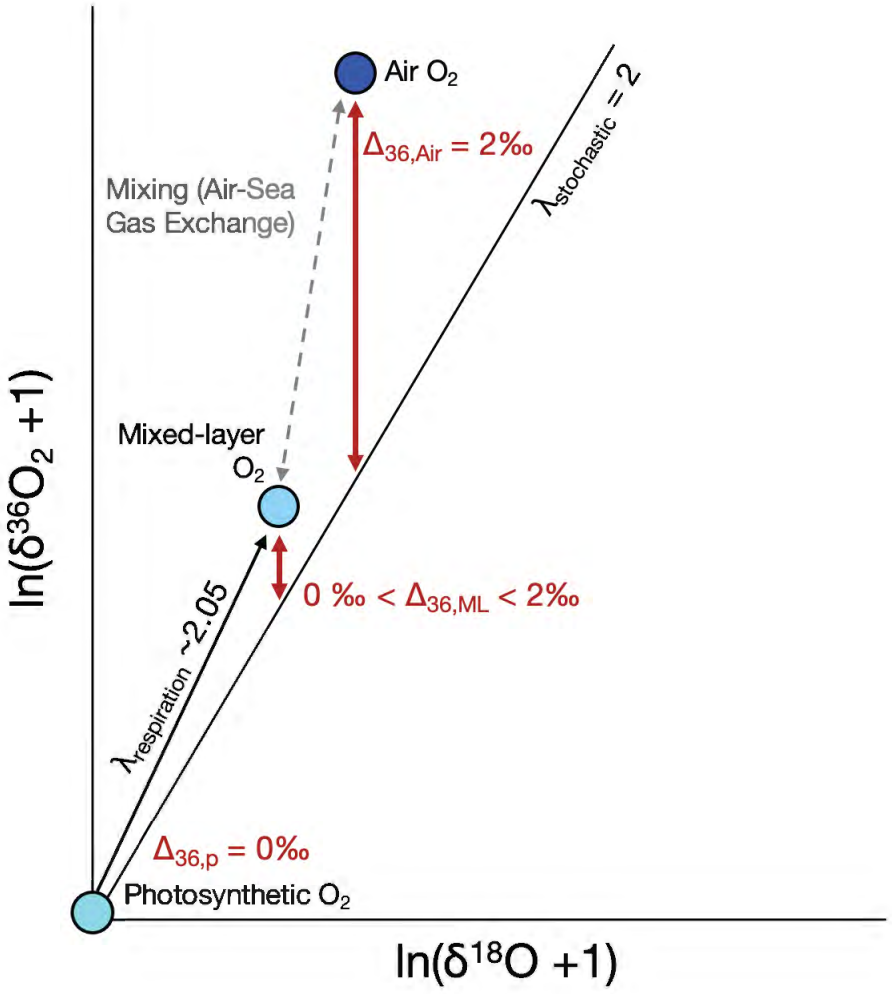

Figure 9. Schematic of the Δ_{36} method to constrain oxygen production. $\Delta_{36,p}$, $\Delta_{36,Air}$, and $\Delta_{36,ML}$ represent the clumped isotope composition of photosynthetic O_2, O_2 in air, and dissolved O_2 in the ocean mixed layer, respectively.

as Helman et al. (2005) and Eisenstadt et al. (2010), we did not re-suspend cells in fresh growth medium prior to each experiment. Rather, *Synechocystis* cultures were directly transferred from Erlenmeyer flasks in the incu-shaker to the reaction vessel.

Conclusion

The results of this study suggest that previous estimates of marine GOP may include over-estimates since the calculations did not incorporate the effect of nitrate limitation stress. The dependence of the fractionation factors of ^{17}O and ^{18}O on nitrate availability also elucidates the importance of the Mehler-like reaction in alleviating intracellular oxidative stress. This result demonstrates how oxygen isotopes are a useful tool for revealing the mechanism of cellular processes. The observed trend in fractionation factors provides isotopic evidence for the potential role played by the Mehler-like reaction in protecting the cell under nitrate limitation. Finally, this study generates new data on the clumped isotope composition of cyanobacterial photosynthetic O_2. The invariance of the Δ_{36} parameter under varying nutrient availability makes it a robust tool for quantifying primary productivity and acting as an additional constraint on marine primary productivity that supplements the TOI method.

Future studies should evaluate the extent of fractionation during photosynthesis carried out by different phytoplankton species and the effect of other forms of stress on isotope fractionation during photosynthesis. Understanding the response of oxygen isotope fractionation to different forms of stress by various species will allow for better constraints on the interpretation of oxygen isotope composition of dissolved O_2 in the ocean. These improved constraints will allow for more accurate quantification of marine oxygen production and primary productivity in the modern ocean. In addition, a better understanding of the photosynthetic endmember of oxygen isotope fractionation may improve the reconstruction of past primary productivity using proxies of marine dissolved oxygen, such as ferromanganese crusts (Sutherland et al., 2020).

Acknowledgements

I would like to thank all those who helped me complete this senior honors thesis. I'm grateful for Dr. Laurence Yeung for giving me the opportunity to work on this project and for his guidance during the process. I appreciate the constant support and mentoring I received from Bing Yuan and Dr. Tao Sun. I would like to thank Dr. Asmita Banerjee, Yi Hou, and Will Larsen for helping with various measurements and teaching me many techniques in the lab. I'm grateful for the guidance and feedback provided by Dr. Mark Torres who oversaw the senior honors thesis program. This project also would not have been possible without the support from Dr. Carrie Masiello and Dr. Xiaodong Gao. I greatly appreciate Dr. Caroline Ajo-Franklin and Bobby Tesoriero who kindly provided the cyanobacteria used in this study and taught me how to inoculate the cultures.

References

Allahverdiyeva, Y., Isojärvi, J., Zhang, P., and Aro, E.-M. (2015). Cyanobacterial Oxygenic Photosynthesis is Protected by Flavodiiron Proteins. *Life*, 5(1):716–743.

Allahverdiyeva, Y., Mustila, H., Ermakova, M., Bersanini, L., Richaud, P., Ajlani, G., Battchikova, N., Cournac, L., and Aro, E.-M. (2013). Flavodiiron proteins Flv1 and Flv3 enable cyanobacterial growth and photosynthesis under fluctuating light. *Proceedings of the National Academy of Sciences*, 110(10):4111–4116.

Andersen, I. M., Williamson, T. J., González, M. J., and Vanni, M. J. (2020). Nitrate, ammonium, and phosphorus drive seasonal nutrient limitation of chlorophytes, cyanobacteria, and diatoms in a hyper-eutrophic reservoir. *Limnology and Oceanography*, 65(5):962–978.

Ash, J. L., Hu, H., and Yeung, L. Y. (2020). What Fractionates Oxygen Isotopes during Respiration? Insights from Multiple Isotopologue Measurements and Theory. *ACS Earth and Space Chemistry*, 4(1):50–66.

Barkan, E. and Luz, B. (2011). The relationships among the three stable isotopes of oxygen in air, seawater and marine photosynthesis. *Rapid Communications in Mass Spectrometry*, 25(16):2367–2369.

Behrenfeld, M. J. and Falkowski, P. G. (1997). Photosynthetic rates derived from satellite-based chlorophyll concentration. *Limnology and Oceanography*, 42(1):1–20.

Bender, M., Orchardo, J., Dickson, M.-L., Barber, R., and Lindley, S. (1999). In vitro O2 fluxes compared with 14C production and other rate terms during the JGOFS Equatorial Pacific experiment. *Deep Sea Research Part I: Oceanographic Research Papers*, 46(4):637–654.

Boswell, K. M., D'Elia, M., Johnston, M. W., Mohan, J. A., Warren, J. D., Wells, R. J. D., and Sutton, T. T. (2020). Oceanographic Structure and Light Levels Drive Patterns of Sound Scattering Layers in a Low-Latitude Oceanic System. *Frontiers in Marine Science*, 7:51.

Capone, D. G., Bronk, D. A., Mulholland, M. R., and Carpenter, E. J. (2008). *Nitrogen in the marine environment*. Academic Press, Burlington, MA.

Carr, M.-E., Friedrichs, M. A., Schmeltz, M., Noguchi Aita, M., Antoine, D., Arrigo, K. R., Asanuma, I., Aumont, O., Barber, R., Behrenfeld, M., Bidigare, R., Buitenhuis, E. T., Campbell, J., Ciotti, A., Dierssen, H., Dowell, M., Dunne, J., Esaias, W., Gentili, B., Gregg, W., Groom, S., Hoepffner, N., Ishizaka, J., Kameda, T., Le Quéré, C., Lohrenz, S., Marra, J., Mélin, F., Moore,

K., Morel, A., Reddy, T. E., Ryan, J., Scardi, M., Smyth, T., Turpie, K., Tilstone, G., Waters, K., and Yamanaka, Y. (2006). A comparison of global estimates of marine primary production from ocean color. *Deep Sea Research Part II: Topical Studies in Oceanography*, 53(5-7):741–770.

Chan, E. (2003). Microbial nutrition and basic metabolism. In *Handbook of Water and Wastewater Microbiology*, pages 3–33. Elsevier.

Eiler, J. M. (2007). "Clumped-isotope" geochemistry—The study of naturally-occurring, multiply-substituted isotopologues. *Earth and Planetary Science Letters*, 262(3-4):309–327.

Eisenstadt, D., Barkan, E., Luz, B., and Kaplan, A. (2010). Enrichment of oxygen heavy isotopes during photosynthesis in phytoplankton. *Photosynthesis Research*, 103(2):97–103.

Elena García-Martín, E., Serret, P., and Pérez-Lorenzo, M. (2011). Testing potential bias in marine plankton respiration rates by dark bottle incubations in the NW Iberian shelf: incubation time and bottle volume. *Continental Shelf Research*, 31(5):496–506.

Flores, E., Frías, J. E., Rubio, L. M., and Herrero, A. (2005). Photosynthetic nitrate assimilation in cyanobacteria. *Photosynthesis Research*, 83(2):117–133.

Flores, E. and Herrero, A. (2005). Nitrogen assimilation and nitrogen control in cyanobacteria. *Biochemical Society Transactions*, 33(1):164–167.

Guy, R. D., Fogel, M. L., and Berry, J. A. (1993). Photosynthetic Fractionation of the Stable Isotopes of Oxygen and Carbon. *Plant Physiology*, 101(1):37–47.

Hale, M. S., Li, W. K., and Rivkin, R. B. (2017). Meridional patterns of inorganic nutrient limitation and co-limitation of bacterial growth in the Atlantic Ocean. *Progress in Oceanography*, 158:90–98.

Helman, Y., Barkan, E., Eisenstadt, D., Luz, B., and Kaplan, A. (2005). Fractionation of the Three Stable Oxygen Isotopes by Oxygen-Producing and Oxygen-Consuming Reactions in Photosynthetic Organisms. *Plant Physiology*, 138(4):2292–2298.

Hill, V. J., Matrai, P. A., Olson, E., Suttles, S., Steele, M., Codispoti, L., and Zimmerman, R. C. (2013). Synthesis of integrated primary production in the Arctic Ocean: II. In situ and remotely sensed estimates. *Progress in Oceanography*, 110:107–125.

Hunt, G. L. and McKinnell, S. (2006). Interplay between top-down, bottom-up, and wasp-waist control in marine ecosystems. *Progress in Oceanography*, 68(2-4):115–124.

Hutchins, D. A. and Fu, F. (2017). Microorganisms and ocean global change. *Nature Microbiology*, 2(6):17058.

Imlay, J. A. (2003). Pathways of Oxidative Damage. *Annual Review of Microbiology*, 57(1):395–418.

Inabe, K., Miichi, A., Matsuda, M., Yoshida, T., Kato, Y., Hidese, R., Kondo, A., and Hasunuma, T. (2021). Nitrogen Availability Affects the Metabolic Profile in Cyanobacteria. *Metabolites*, 11(12):867.

Juranek, L. and Quay, P. (2013). Using Triple Isotopes of Dissolved Oxygen to Evaluate Global Marine Productivity. *Annual Review of Marine Science*, 5(1):503–524.

Klotz, A., Reinhold, E., Doello, S., and Forchhammer, K. (2015). Nitrogen Starvation Acclimation in Synechococcus elongatus: Redox-Control and the Role of Nitrate Reduction as an Electron Sink. *Life*, 5(1):888–904.

Krasikov, V., Aguirre von Wobeser, E., Dekker, H. L., Huisman, J., and Matthijs, H. C. P. (2012). Time-series resolution of gradual nitrogen starvation and its impact on photosynthesis in the cyanobacterium Synechocystis PCC 6803. *Physiologia Plantarum*, 145(3):426–439.

Lea-Smith, D. J., Bombelli, P., Vasudevan, R., and Howe, C. J. (2016). Photosynthetic, respiratory and extracellular electron transport pathways in cyanobacteria. *Biochimica et Biophysica Acta (BBA) - Bioenergetics*, 1857(3):247–255.

Lee, Z., Marra, J., Perry, M. J., and Kahru, M. (2015). Estimating oceanic primary productivity from ocean color remote sensing: A strategic assessment. *Journal of Marine Systems*, 149:50–59.

Li, Q., Legendre, L., and Jiao, N. (2015). Phytoplankton responses to nitrogen and iron limitation in the tropical and subtropical Pacific Ocean. *Journal of Plankton Research*, 37(2):306–319.

Luz, B. and Barkan, E. (2000). Assessment of Oceanic Productivity with the Triple-Isotope Composition of Dissolved Oxygen. *Science*, 288(5473):2028–2031.

Luz, B. and Barkan, E. (2005). The isotopic ratios 17O/16O and 18O/16O in molecular oxygen and their significance in biogeochemistry. *Geochimica et Cosmochimica Acta*, 69(5):1099–1110.

Luz, B. and Barkan, E. (2009). Net and gross oxygen production from O2/Ar, 17O/16O and 18O/16O ratios. *Aquatic Microbial Ecology*, 56:133–145.

Luz, B., Barkan, E., Bender, M. L., Thiemens, M. H., and Boering, K. A. (1999). Triple-isotope composition of atmospheric oxygen as a tracer of biosphere productivity. *Nature*, 400(6744):547–550.

Marra, J. (2009). Net and gross productivity: weighing in with 14C. *Aquatic Microbial Ecology*, 56:123–131.

Moon, J. and Carrick, H. (2007). Seasonal variation of phytoplankton nutrient limitation in Lake Erie. *Aquatic Microbial Ecology*, 48:61–71.

Muramatsu, M. and Hihara, Y. (2012). Acclimation to high-light conditions in cyanobacteria: from gene expression to physiological responses. *Journal of Plant Research*, 125(1):11–39.

Nielsen, E. S. (1952). The Use of Radio-active Carbon (C14) for Measuring Organic Production in the Sea. *ICES Journal of Marine Science*, 18(2):117–140.

Nowicki, M., DeVries, T., and Siegel, D. A. (2022). Quantifying the Carbon Export and Sequestration Pathways of the Ocean's Biological Carbon Pump. *Global Biogeochemical Cycles*, 36(3).

Prokopenko, M. G., Pauluis, O. M., Granger, J., and Yeung, L. Y. (2011). Exact evaluation of gross photosynthetic production from the oxygen triple-isotope composition of O_2 : Implications for the net-to-gross primary production ratios. *Geophysical Research Letters*, 38(14):n/a–n/a.

Quay, P. D., Peacock, C., Björkman, K., and Karl, D. M. (2010). Measuring primary production rates in the ocean: Enigmatic results between incubation and non-incubation methods at Station ALOHA. *Global Biogeochemical Cycles*, 24(3):n/a–n/a.

Rachedi, R., Foglino, M., and Latifi, A. (2020). Stress Signaling in Cyanobacteria: A Mechanistic Overview. *Life*, 10(12):312.

Salomon, E., Bar-Eyal, L., Sharon, S., and Keren, N. (2013). Balancing photosynthetic electron flow is critical for cyanobacterial acclimation to nitrogen limitation. *Biochimica et Biophysica Acta (BBA) - Bioenergetics*, 1827(3):340–347.

Saroussi, S., Sanz-Luque, E., Kim, R. G., and Grossman, A. R. (2017). Nutrient scavenging and energy management: acclimation responses in nitrogen and sulfur deprived Chlamydomonas. *Current Opinion in Plant Biology*, 39:114–122.

Sigman, D. M. and Boyle, E. A. (2000). Glacial/interglacial variations in atmospheric carbon dioxide. *Nature*, 407(6806):859–869.

Stanier, R. Y., Kunisawa, R., Mandel, M., and Cohen-Bazire, G. (1971). Purification and properties of unicellular blue-green algae (order Chroococcales). *Bacteriological Reviews*, 35(2):171–205.

Sutherland, K. M., Johnston, D. T., Hemingway, J. D., Wankel, S. D., and Ward, C. P. (2022). Revised microbial and photochemical triple-oxygen isotope effects improve marine gross oxygen production estimates. *PNAS Nexus*, page pgac233.

Sutherland, K. M., Wostbrock, J. A., Hansel, C. M., Sharp, Z. D., Hein, J. R., and Wankel, S. D.

(2020). Ferromanganese crusts as recorders of marine dissolved oxygen. *Earth and Planetary Science Letters*, 533:116057.

Ustick, L. J., Larkin, A. A., Garcia, C. A., Garcia, N. S., Brock, M. L., Lee, J. A., Wiseman, N. A., Moore, J. K., and Martiny, A. C. (2021). Metagenomic analysis reveals global-scale patterns of ocean nutrient limitation. *Science*, 372(6539):287–291.

van Geldern, R. and Barth, J. A. (2012). Optimization of instrument setup and post-run corrections for oxygen and hydrogen stable isotope measurements of water by isotope ratio infrared spectroscopy (IRIS): Water stable isotope analysis with IRIS. *Limnology and Oceanography: Methods*, 10(12):1024–1036.

Yamamoto, A., Abe-Ouchi, A., and Yamanaka, Y. (2018). Long-term response of oceanic carbon uptake to global warming via physical and biological pumps. *Biogeosciences*, 15(13):4163–4180.

Yeung, L. Y. (2016). Combinatorial effects on clumped isotopes and their significance in biogeochemistry. *Geochimica et Cosmochimica Acta*, 172:22–38.

Yeung, L. Y., Ash, J. L., and Young, E. D. (2014). Rapid photochemical equilibration of isotope bond ordering in O $_2$: Photochemical isotope reordering in O2. *Journal of Geophysical Research: Atmospheres*, 119(17):10552–10566.

Yeung, L. Y., Ash, J. L., and Young, E. D. (2015). Biological signatures in clumped isotopes of O $_2$. *Science*, 348(6233):431–434.

Yeung, L. Y., Hayles, J. A., Hu, H., Ash, J. L., and Sun, T. (2018). Scale distortion from pressure baselines as a source of inaccuracy in triple-isotope measurements. *Rapid Communications in Mass Spectrometry*, 32(20):1811–1821.

Young, E. D., Yeung, L. Y., and Kohl, I. E. (2014). On the 17O budget of atmospheric O2. *Geochimica et Cosmochimica Acta*, 135:102–125.